Computational fluid dynamics and thermodynamic analysis of transport and reaction phenomena in autothermal reforming reactors for hydrogen production

Junjie Chen [a, b, *]

[a] Department of Mechanical and Aerospace Engineering, College of Engineering, University of California, Davis, California, 95616, United States

[b] Department of Energy and Power Engineering, School of Mechanical and Power Engineering, Henan Polytechnic University, Jiaozuo, Henan, 454000, P.R. China

* Corresponding author, E-mail address: junjiem@tom.com

Abstract

Computational fluid dynamics uses numerical methods and algorithms to solve and analyse problems that involve fluid flows. Computers may be used to perform the calculations required to simulate the interaction of liquids and gasses with a surface defined by boundary conditions. Thermodynamics is the science of the relationship between heat, work, temperature, and energy. Computational modelling for microchannel reactor design was performed to investigate the effects of various factors on the efficiency and performance of an autothermal reforming system. The yield and productivity from the chemical process were determined by performing computational fluid dynamics and thermodynamic analysis. Strength and weakness were assessed under different reaction conditions. Design recommendations were provided and operation strategies were mapped out. The results indicated that operation at millisecond contact times is feasible, but optimisation of reaction conditions is necessary to balance efficiency and performance. The conversion to hydrogen is influenced greatly by the feed composition, which must be controlled precisely within certain needed limits to maximize the yield and productivity from the autothermal reforming process while avoiding the problems of combustion or explosion. Additionally, the efficiency difference between feed compositions is determined by thermodynamic analysis. The calculated output power of the autothermal reforming reactor is of the order of thousands of kilowatts per cubic meter.

Keywords: Autothermal reforming; Hydrogen production; Output power; Steam reforming; Transport phenomena; Reaction phenomena

1. Introduction

Conventional energy sources emit significant amounts of greenhouse gases, thus prompting a growing emphasis on clean energy solutions [1, 2]. Hydrogen energy has emerged as an ideal alternative due to its abundant sources [3, 4], high combustion calorific value, absence of pollution, and production of only water during the combustion process, rendering it environmentally friendly. The production of hydrogen can be primarily achieved through three methods: fossil fuel-based hydrogen production [5, 6], electrolytic water-based hydrogen production [7, 8], and renewable source-based hydrogen production. Methanol serves as a promising raw material for extracting hydrogen from fossil fuels owing to its favourable reaction conditions, low likelihood of carbon deposition reactions, and absence of sulphur in liquid form [9, 10]. Consequently, methanol has garnered considerable attention as one of the focal points.

Fuel cells [11, 12], as the fourth-generation technology succeeding thermal power generation [13, 14], hydroelectric power generation [15, 16], and atomic power generation, are a chemical device that efficiently converts chemical energy into electrical energy without the need for mechanical transmission. It possesses remarkable advantages such as high efficiency, zero noise pollution, and zero

environmental impact compared to traditional power generation technologies [17, 18]. Consequently, fuel cells are widely recognized as one of the most promising energy sources from both an energy conservation and environmental protection perspective [19, 20]. Compared to other types of fuel cells, proton exchange membrane fuel cells have garnered significant attention due to their characteristics such as low operating temperature, excellent stability, rapid response speed, and high-power density [21, 22]. They have gained widespread recognition in the automotive, trucking, maritime, and aerospace industries. To address the hydrogen supply for proton exchange membrane fuel cells, three direct storage methods are primarily employed: metal hydride storage, low-temperature liquid storage, and high-pressure gas storage [23, 24]. However, these approaches present certain challenges including inadequate security measures, high-cost implications, and low storage density. Consequently, hydrogen supply remains a major obstacle hindering the advancement of fuel cell technology. A viable solution to this predicament lies in small-scale methanol reforming for on-site hydrogen production.

According to various reaction mechanisms and condition, hydrogen production from methanol reforming can be categorized into three pathways: methanol steam reforming [9, 10], methanol partial oxidation reforming [25, 26], and methanol autothermal reforming [27, 28]. Among these, the autothermal reforming of methanol is achieved by combining partial oxidation reforming with combustion reaction. By precisely adjusting the water-to-alcohol ratio, thermal equilibrium of the reaction can be attained, thereby maintaining a stable operating temperature without requiring an external heat source. Since the reforming process necessitates substantial heat energy absorption, the provision of heat and thermal management in the reactor significantly impact its performance. The traditional macroscopic methanol reforming hydrogen production reactor suffers from low efficiency [29, 30], limited fluid flow and mass transfer due to channel size, resulting in poor uniformity. In contrast, microchannel hydrogen production reactors offer larger surface area, enhanced transfer capacity, and portability [31, 32]. Designing a microreactor requires the comprehensive application of multidisciplinary knowledge as it is a complex microscale system.

Given that methanol reforming is an endothermic reaction, adequate external heating equipment is necessary in the design process. Therefore, current advanced design concepts for microscale reactors primarily focus on the spontaneous generation of required heating equipment and coupling the incineration channel with the reforming channel to enhance device portability [33, 34]. Improvements mainly involve optimizing catalyst preparation methods, adjusting reaction materials, and modifying the size and shape of the reforming channels to improve efficiency. Additionally, advantages such as increasing specific surface area and facilitating transfer processes are achieved by adjusting and arranging them into a micro-channel configuration [35, 36]. The reactor employs thermal absorption and exothermic coupling treatment to facilitate catalytic combustion and methanol reforming reactions, thereby supplying the necessary heat for hydrogen production through adjacent reaction heat exchange [35, 36]. This design enhances the compactness of the arrangement and improves reactor portability. All thermal absorption and exothermic reactions within the reactor are catalytic in nature, with their reaction rates directly influencing the thermal effect of the reactor. Factors affecting reaction speed and final product yield, such as reaction temperature and reactant concentration, can be utilized to regulate temperature distribution and enhance catalyst utilization rate [37, 38]. By employing a fixed amount of catalyst or reducing catalyst usage while maintaining certain export products, higher conversion rates can be achieved along with reduced catalyst requirements and cost savings [37, 38]. These findings hold significant implications for precious metal catalysts.

While substantial effort has been made to preparate and characterise of autothermal reforming catalysts but provide no insight into the transport phenomena involved. In particular, little research has been conducted to understand and optimise the physical and chemical processes in millisecond microchannel reactors, in which it may be impossible to simultaneously achieve high efficiency and

performance. In the present study, computational modelling for microchannel reactor design was conducted in the attempt to fully understand autothermal reforming phenomena in continuous flow reactors. The effects of various factors on the efficiency and performance were evaluated by performing computational fluid dynamics and thermodynamic analysis under different design conditions. The reactor efficiency and performance were assessed by means of the reactant conversion, product yield, reaction rate, hydrogen productivity, and output power. Thermodynamic analysis was carried out in terms of enthalpy, sensible enthalpy, and entropy. Recommendations for designing an autothermal reforming system were made and strategies for performing efficient operation were set forth. The present study aims to understand and optimise the autothermal reforming process in a millisecond microchannel reactor. Particular emphasis is placed upon the effects of various factors on the efficiency and performance of the reactor system. The subject has numerous applications in fields varying from hydrogen production to the study of flow in microchannel reactors.

2. Reactor model

2.1. Reactor geometry and operation conditions

A typical fuel processor may use an autothermal reforming reactor as a primary reactor to initiate the production of the hydrogen-containing reformate stream. Autothermal reforming reactors introduce reactants into the front of the reactor and allow the associated reactions to occur to completion as the reactants flow through the reactor. The fuel can come in a variety of forms. The oxidant is typically provided in the form of oxygen or air. The steam is typically superheated steam which supplies heat and water to the reactor. An autothermal reforming reactor is capable of converting the fuel into a nitrogen or steam diluted reformate stream containing hydrogen and carbon oxides that result from the combined partial oxidation reaction and steam reforming reaction, the extent of each being dependant on the operating conditions, for example, availability of an oxidant and steam and temperature of the reactor. A steam reformer may also serve as the primary reactor which eliminates the nitrogen diluent that is present when partial oxidation is also included as in autothermal reforming. These two different reactions differ in their efficiencies, the operating conditions that increase and maximize the efficiencies, and their ability to quickly adjust to transient changes in the demand for the hydrogen-containing reformate stream. For example, the steam reforming reaction is typically more efficient at producing the hydrogen-containing reformate stream than the partial oxidation reaction. Additionally, the steam reforming reaction is more efficient at higher pressures. The partial oxidation reaction is able to respond more quickly to transient changes in the demand for the hydrogen-containing reformate stream than the steam reforming reaction.

A microchannel reactor is utilized to continuously produce hydrogen by auto-thermally reforming a methanol feed. The chemical method can increase the hydrogen yield due to simultaneous catalytic partial oxidation and steam reforming being attained. The reactor in which the autothermal reforming reaction of methanol is carried out is illustrated schematically in Figure 1 with the wall and washcoat indicated. The catalyst washcoat coating, in which the reaction proceeds, is applied onto the interior surface of the stainless-steel wall of the square channel. Unless otherwise specified, the coating is 0.10 mm in thickness, the wall is 0.20 mm in thickness, the channels are 0.7 mm in height, and the flowthrough path is 50.0 mm in length. Difficulties associated with the production of hydrogen from methane or natural gas, for example, high temperatures and pressures, favour the use of methanol. Advantageously, high temperatures are not required to carry the reaction to completion within certain ranges of operation conditions. The heat loss is negligible if the number of channels is sufficient large. In the autothermal reforming process, fuel, steam and preheated air are mixed and passed over the catalyst surface. The air is added to the reactants to raise the temperature of the reactants and supply the

endothermic heat for reaction. Unless otherwise noted, the feed contains methanol, steam, and oxygen in a molar ratio of methanol to steam of 100:100 and in a molar ratio of methanol to oxygen of 100:23 with oxygen as the limiting reactant, such that the oxygen concentration is minimal on the catalyst surface. The reactor operates with an inlet velocity of 2.0 m/s and with an inlet temperature of 100 °C at one atmosphere pressure, whereupon the reaction proceeds by the contact time in milliseconds. The catalyst converts methanol to a mixture of mostly hydrogen and carbon dioxide gases. The reaction product mixture flows from the reactor for further processing and utilization. At operation temperatures, conventional steam reforming catalysts such as nickel on alpha alumina are deficient in activity.

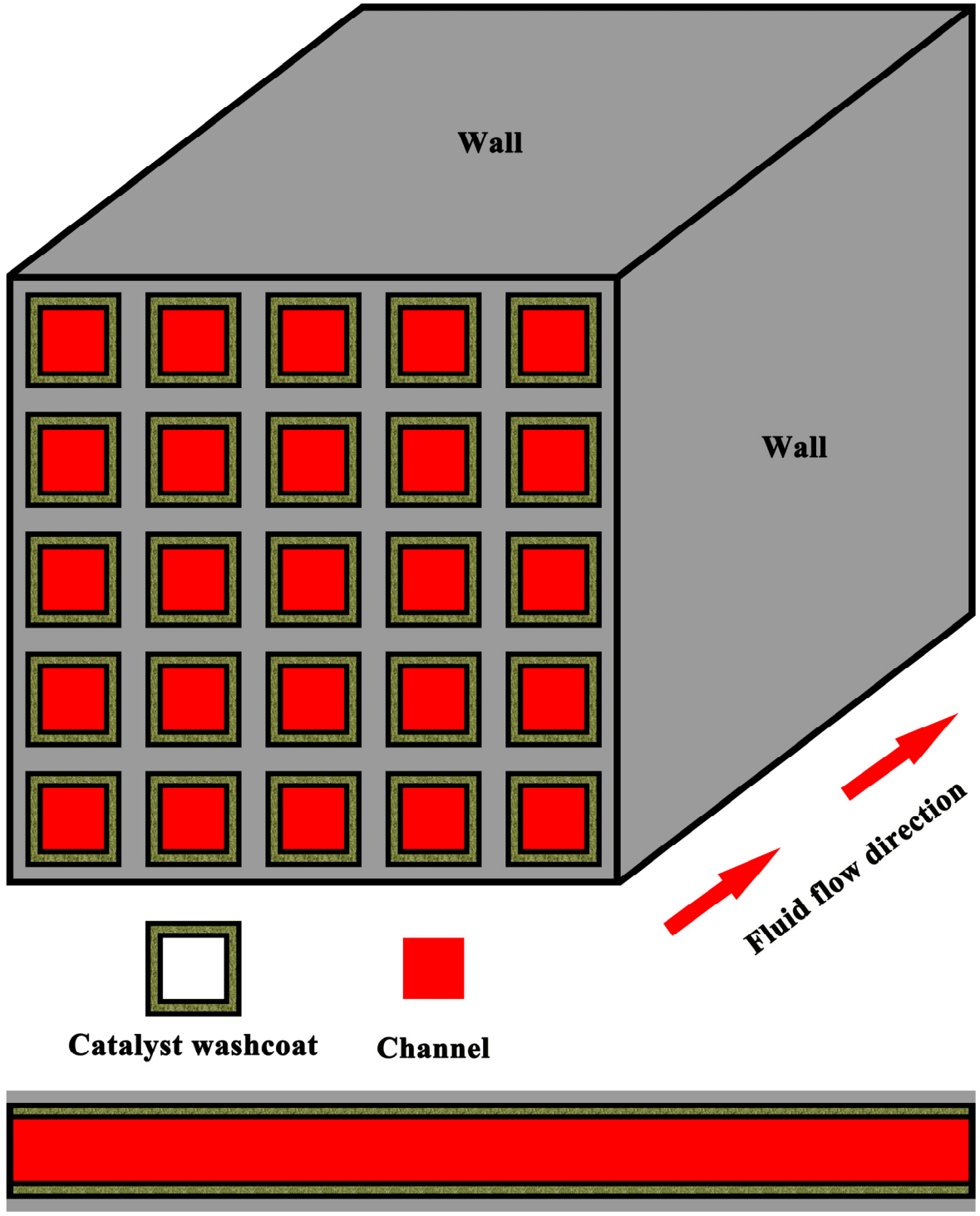

Figure 1. Illustration representation of the microchannel reactor for the production of hydrogen by autothermal reforming of methanol with the fluid flow direction indicated. The reactor may contain any desired number of channels.

2.2. Conservation equations

In the gas phase, mathematically, momentum and species conservation equations are solved

$$\begin{aligned}&\frac{\partial}{\partial x}\left[\mu\left(\frac{\partial u_x}{\partial x}+\frac{\partial u_x}{\partial x}\right)\right]+\frac{\partial}{\partial y}\left[\mu\left(\frac{\partial u_x}{\partial y}+\frac{\partial u_y}{\partial x}\right)\right]+\frac{\partial}{\partial z}\left[\mu\left(\frac{\partial u_x}{\partial z}+\frac{\partial u_z}{\partial x}\right)\right]\\&-\frac{\partial}{\partial x}\left[\frac{2}{3}\mu\left(\frac{\partial u_{xx}}{\partial x}+\frac{\partial u_{yx}}{\partial y}+\frac{\partial u_{zx}}{\partial z}\right)\right]-\frac{\partial p}{\partial x}=0\end{aligned}, \tag{1}$$

$$\begin{aligned}&\frac{\partial}{\partial x}\left[\mu\left(\frac{\partial u_y}{\partial x}+\frac{\partial u_x}{\partial y}\right)\right]+\frac{\partial}{\partial y}\left[\mu\left(\frac{\partial u_y}{\partial y}+\frac{\partial u_y}{\partial y}\right)\right]+\frac{\partial}{\partial z}\left[\mu\left(\frac{\partial u_y}{\partial z}+\frac{\partial u_z}{\partial y}\right)\right]\\&-\frac{\partial}{\partial y}\left[\frac{2}{3}\mu\left(\frac{\partial u_{xy}}{\partial x}+\frac{\partial u_{yy}}{\partial y}+\frac{\partial u_{zy}}{\partial z}\right)\right]-\frac{\partial p}{\partial y}=0\end{aligned}, \tag{2}$$

$$\begin{aligned}&\frac{\partial}{\partial x}\left[\mu\left(\frac{\partial u_z}{\partial x}+\frac{\partial u_x}{\partial z}\right)\right]+\frac{\partial}{\partial y}\left[\mu\left(\frac{\partial u_z}{\partial y}+\frac{\partial u_y}{\partial z}\right)\right]+\frac{\partial}{\partial z}\left[\mu\left(\frac{\partial u_z}{\partial z}+\frac{\partial u_z}{\partial z}\right)\right]\\&-\frac{\partial}{\partial z}\left[\frac{2}{3}\mu\left(\frac{\partial u_{xz}}{\partial x}+\frac{\partial u_{yz}}{\partial y}+\frac{\partial u_{zz}}{\partial z}\right)\right]-\frac{\partial p}{\partial z}=0\end{aligned}, \tag{3}$$

$$\frac{\partial\left(\rho u_x w_k\right)}{\partial x}+\frac{\partial\left(\rho u_y w_k\right)}{\partial y}+\frac{\partial\left(\rho u_z w_k\right)}{\partial z}+\frac{\partial}{\partial x}\left(\rho w_k V_{k,x}\right)+\frac{\partial}{\partial y}\left(\rho w_k V_{k,y}\right)+\frac{\partial}{\partial z}\left(\rho w_k V_{k,z}\right)=0, \tag{4}$$

$$\vec{V}_g=-D_g^m\nabla\left(\ln\left(\frac{Y_g M'}{M_g}\right)\right)+\left(\frac{D_g^T M_g}{\rho Y_g M'}\right)\nabla\left(\ln T\right), \tag{5}$$

wherein the subscripts x, y, and z refer to coordinate variables, the subscript x also refers to the streamwise distance, the subscripts y and z also refer to the transverse distance, the subscripts k and g refers to the gas-phase species and gas mixture, respectively, and u, ρ, w, p, V, T, μ, M, M', D^m, and D^T are the velocity, density, mass fraction, pressure, diffusion velocity, temperature, dynamic viscosity, molecular weight, mean molecular weight, transport coefficient that describes molecular diffusion, and transport coefficient that describes thermal diffusion, respectively.

In the gas phase, energy and mass conservation equations are solved

$$\begin{aligned}&\frac{\partial\left(\rho u_x h\right)}{\partial x}+\frac{\partial\left(\rho u_y h\right)}{\partial y}+\frac{\partial\left(\rho u_z h\right)}{\partial z}+\frac{\partial}{\partial x}\left(\rho\sum_{k=1}^{\gamma}w_k h_k V_{k,x}-\kappa_g\frac{\partial T}{\partial x}\right)+\frac{\partial}{\partial y}\left(\rho\sum_{k=1}^{\gamma}w_k h_k V_{k,y}-\kappa_g\frac{\partial T}{\partial y}\right)\\&+\frac{\partial}{\partial z}\left(\rho\sum_{k=1}^{\gamma}w_k h_k V_{k,z}-\kappa_g\frac{\partial T}{\partial z}\right)=0\end{aligned}, \tag{6}$$

$$\frac{\partial\left(\rho u_x\right)}{\partial x}+\frac{\partial\left(\rho u_y\right)}{\partial y}+\frac{\partial\left(\rho u_z\right)}{\partial z}=0, \tag{7}$$

$$p=\frac{\rho}{M'}RT, \tag{8}$$

$$h_k\left(T\right)=h_k\left(298.15\text{ K}\right)+\int_{298.15\text{ K}}^{T}c_{p,k}dT, \tag{9}$$

wherein κ and h are the thermal conductivity and enthalpy, respectively, γ denotes the total number of gas-phase species, R is the perfect gas constant, and c_p is specific heat capacity.

Heat diffuses in the coating via conduction [39, 40], and the rate of energy transfer depends upon the effective thermal conductivity of the porous material involved [41, 42]

$$\frac{\partial}{\partial x}\left(\kappa'\frac{\partial T}{\partial x}\right)+\frac{\partial}{\partial y}\left(\kappa'\frac{\partial T}{\partial y}\right)+\frac{\partial}{\partial z}\left(\kappa'\frac{\partial T}{\partial z}\right)=0, \tag{10}$$

$$\kappa'=\left(1-\varepsilon_p\right)\kappa_s+\varepsilon_p\kappa_g, \tag{11}$$

in which κ' is the effective thermal conductivity and κ_s is the solid phase thermal conductivity.

A species coverage equation is solved on the catalyst surface

$$\frac{\theta_m\dot{r}_m}{\Gamma}=0, \quad m=1,\ldots,\gamma', \tag{12}$$

wherein θ, r, γ', and Γ is the coverage, reaction rate, total number of surface species, and site density, respectively, and the subscript m refers to the surface species.

The effective gaseous diffusivity is determined by

$$\frac{1}{D_i'}=\tau_p\frac{1}{\varepsilon_p}\left(\frac{1}{D_i^m}+\frac{1}{D_i^K}\right), \tag{13}$$

$$D_i^K=\frac{d}{3}\left(8RT\right)^{\frac{1}{2}}\left(\pi W_i\right)^{-\frac{1}{2}}, \tag{14}$$

wherein D', d, τ_p, ε_p, and D^K are the effective gaseous diffusivity, mean pore diameter, tortuosity, porosity, and Knudsen diffusivity.

Energy and gas-phase species conservation equations are solved at the fluid-coating interface

$$\kappa_s\left(\frac{\partial T}{\partial y}\right)_{\Omega+}-\kappa_g\left(\frac{\partial T}{\partial y}\right)_{\Omega-}+\kappa_s\left(\frac{\partial T}{\partial z}\right)_{\Omega+}-\kappa_g\left(\frac{\partial T}{\partial z}\right)_{\Omega-}+\sum_{k=1}^{K_g}\left(\dot{r}_k h_k W_k\right)_\Omega=0. \tag{15}$$

$$\eta\lambda M_k\left(\dot{r}_k\right)_\Theta+\left(\rho w_k V_{k,y\text{ or }z}\right)_\Theta=0, \; k=1,\ldots,K_g. \tag{16}$$

$$\lambda=\frac{A_i}{A_e}, \tag{17}$$

wherein the subscript Θ refers to the fluid-coating interface, and λ is the surface area factor, A_i is the interior surface area of the coating, and A_e is the exterior or geometric surface area exposed to the reactant gases, and η is the effectiveness factor.

The effectiveness factor is determined by

$$\eta_g=\frac{\dot{r}_g'}{\dot{r}_g}=\frac{\tanh\left(\Phi\right)}{\Phi}, \tag{18}$$

$$\Phi=\delta\sqrt{\frac{S\dot{r}_g}{C_g D_g}}, \tag{19}$$

in which $\dot{r}'$, Φ, C, S, and δ are the effective reaction rate, Thiele modulus, concentration, specific surface area of the coating, and thickness of the coating, respectively.

3. Results and discussion

The three-dimensional contour maps of temperature and species mole fraction in the reactor are illustrated in Figure 2 with the channel and washcoat indicated. The feed mixture has an oxygen-methanol molar ratio of 0.23 with oxygen as the limiting reactant, and the reaction occurs

under conditions of nearly constant atmospheric pressure, unless otherwise specified. The ratio of reactants and products in the autothermal reforming reaction is called chemical stoichiometry. Stoichiometry depends on the fact that matter is conserved in chemical processes, and calculations giving mass relationships are based on the concept of the mole. Energy plays a key role in the chemical process. Energy is absorbed to break bonds, and energy is evolved as bonds are made. In the reactions, the energy required to break bonds may be larger than the energy evolved on making new bonds, and the net result is the absorption of energy. In an exothermic reaction, energy as heat is evolved. Nearly isothermal operation is achieved in the vast majority of the catalyst washcoat coating. The reaction proceeds at the desired temperatures, and hence the conversion is possible at a sufficiently high rate. While steam is present in excess, oxygen is consumed completely. The chemical reaction can be considered to be completed. Accordingly, operation of the reactor is feasible at millisecond contact times. There is a large amount of carbon dioxide accompanying the reaction, as the concentration of carbon monoxide can be reduced effectively by the water-gas shift reaction.

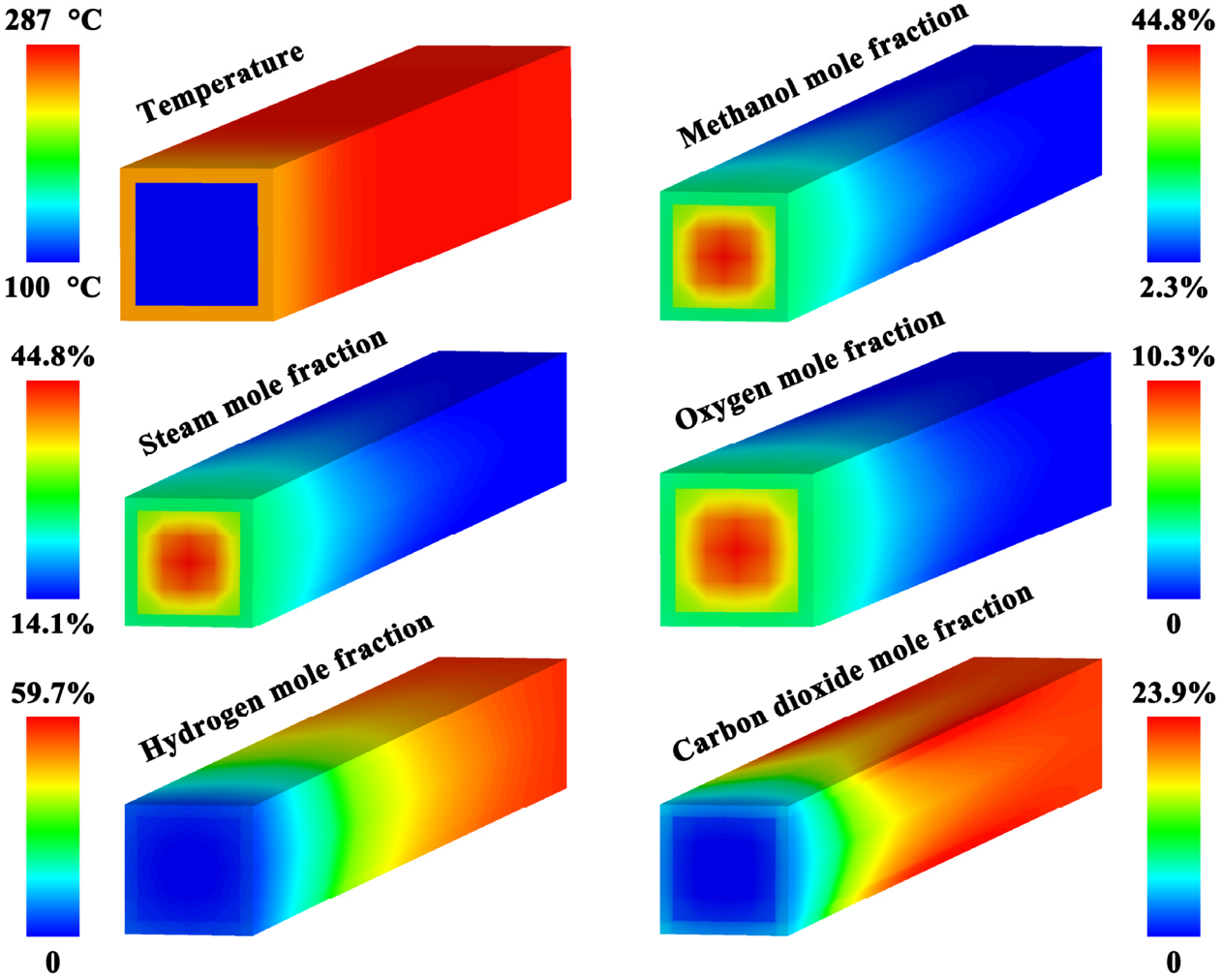

Figure 2. Three-dimensional contour maps of temperature and species mole fraction in the reactor with the channel and washcoat indicated.

The two-dimensional contour maps of methanol mole fraction in the reactor are illustrated in Figure 3 with the feed mixture at different molar ratios of oxygen to methanol. The feed mixture has an oxygen-methanol molar ratio of no greater than 0.25. There occurs a diffusion of reactant molecules down their concentration gradient from the bulk fluid phase to the catalyst surface. The reaction rate depends upon the chemical nature of the species, and the composition of the feed, for example, the molar ratio of oxygen to methanol. The reaction rate is the speed at which the autothermal reforming reaction proceeds. The reaction rate is often expressed in terms of either the concentration of a product

that is formed in a unit of time or the concentration of a reactant that is consumed in a unit of time. Alternatively, it may be defined in terms of the amounts of the reactants consumed or products formed in a unit of time. Chemical reactions proceed at vastly different speeds depending on the nature of the reacting substances, the type of chemical transformation, the temperature, and other factors. For the autothermal reforming reaction, the speed of the reaction will vary with the temperature, the pressure, and the amounts of reactants present. The autothermal reforming reaction usually slows down as time goes on because of the depletion of the reactants. In some cases, the addition of a substance that is not itself a reactant, called a catalyst, accelerates the autothermal reforming reaction. In general, catalytic action is a chemical reaction between the catalyst and a reactant, forming chemical intermediates that are able to react more readily with each other or with another reactant, to form the desired end product. During the reaction between the chemical intermediates and the reactants, the catalyst is regenerated. The rate constant, or the specific rate constant, is the proportionality constant in the equation that expresses the relationship between the rate of a chemical reaction and the concentrations of the reacting substances. The reaction over the catalyst surface is extremely rapid at the temperatures involved, and consequently operation of the reactor is feasible at millisecond contact times. The autothermal reforming reaction is accelerated by a high molar ratio of oxygen to methanol, and therefore the maximum conversion of methanol to hydrogen is attained. At lower molar ratios of oxygen to methanol, the autothermal reforming reaction still occurs rapidly over the catalyst surface but the conversion to hydrogen is incomplete.

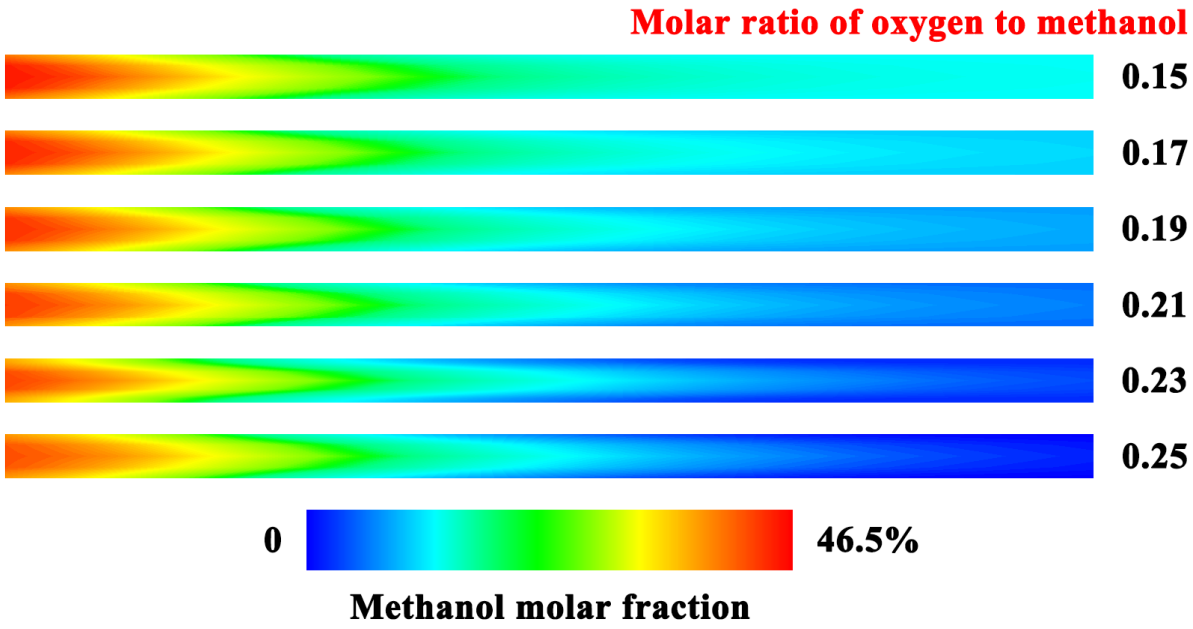

Figure 3. Two-dimensional contour maps of methanol mole fraction in the reactor with the feed mixture at different molar ratios of oxygen to methanol.

The methanol and hydrogen mole fraction profiles along the channel centreline are presented in Figure 4 under different oxygen-methanol molar ratio conditions. The chemical process is self-sustaining, but it may depend heavily upon the feed composition for its success [43, 44]. While methanol undergoes simultaneous chemical reactions that yield different products, the conversion to hydrogen is influenced by the molar ratio of oxygen to methanol. As the oxygen-methanol molar ratio is increased, the methanol mole fraction steadily decreases and the hydrogen mole fraction increases in an almost linear fashion. At the highest molar ratio of oxygen to methanol, the conversion is almost complete. However, equilibrium is not attained, as the methanol mole fraction is still slightly decreased near the exit of the reactor. Chemical equilibrium is the condition in the course of a reversible chemical reaction in which no net change in the amounts of reactants and products occurs. At equilibrium, the

two opposing reactions go on at equal rates, or velocities, and hence there is no net change in the amounts of substances involved. At this point the reaction may be considered to be completed, and the maximum conversion of reactants to products has been attained. By methods of statistical mechanics and chemical thermodynamics, the equilibrium constant is related to the change in the thermodynamic quantity called the standard Gibbs free energy accompanying the reaction. The standard Gibbs free energy of the reaction, which is the difference between the sum of the standard free energies of the products and that of the reactants, is equal to the negative natural logarithm of the equilibrium constant multiplied by the ideal gas constant and the absolute temperature. The equation allows the calculation of the equilibrium constant, or the relative amounts of products and reactants present at equilibrium, from measured or derived values of standard free energies of substances.

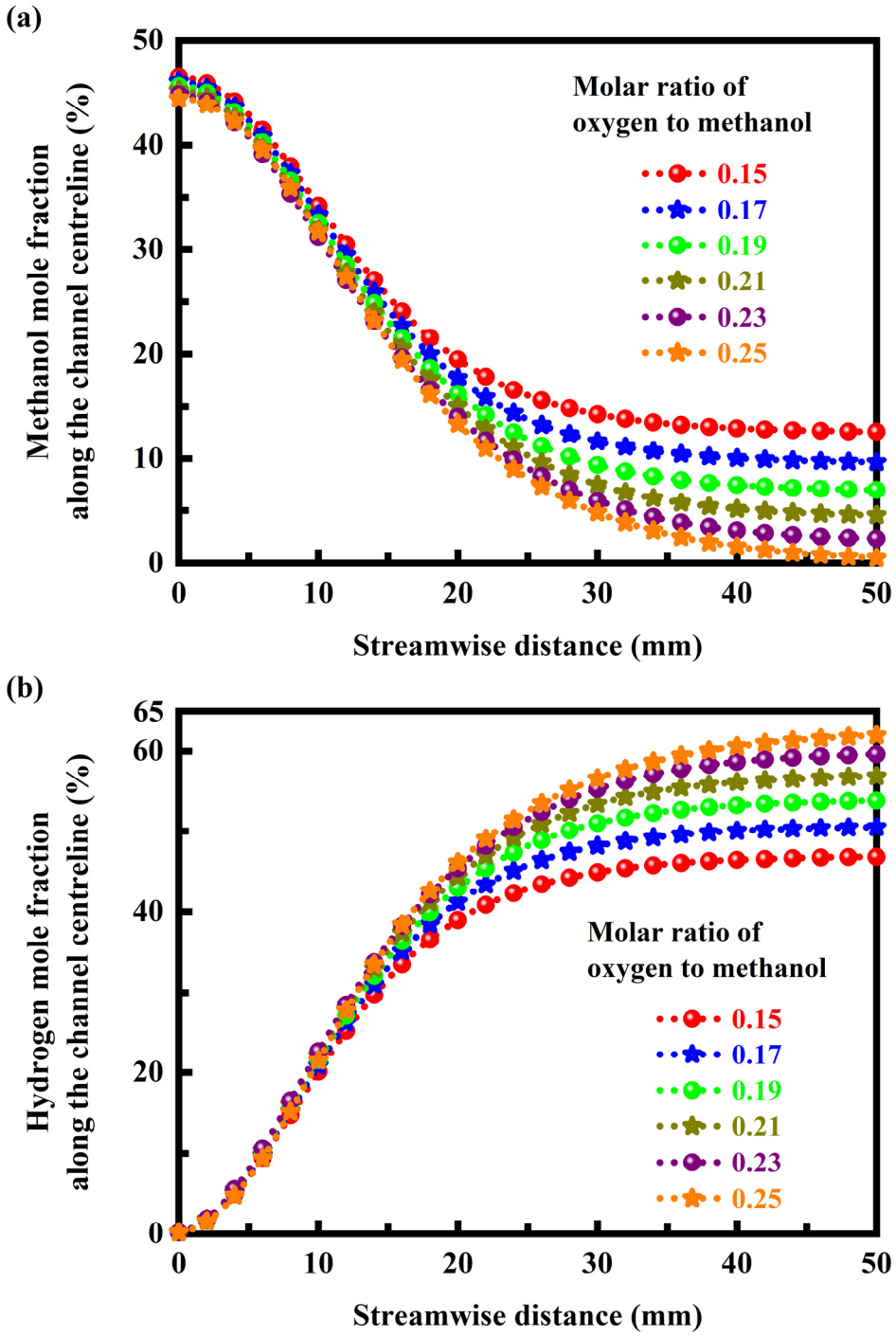

Figure 4. (a) Effect of the molar ratio of oxygen to methanol on the methanol mole fraction along the channel centreline. (b) Effects of the molar ratio of oxygen to methanol on the hydrogen mole fraction along the channel centreline.

The effects of the molar ratio of oxygen to methanol on the methanol conversion, hydrogen yield, and hydrogen productivity of the reactor are illustrated in Figure 5 wherein the results obtained for output power are also presented. The hydrogen productivity is defined in terms of the amount of hydrogen produced in a unit of reactor volume and in a unit of time. Additionally, the output power is calculated based upon the net calorific value of hydrogen at room temperature. At lower molar ratios of oxygen to methanol, there occurs fuel breakthrough or slip, which leads disadvantageously to incomplete conversion, whereupon methanol is converted inefficiently to hydrogen with lower product yields [45, 46]. Higher molar ratios of oxygen to methanol allow for the reactor to reduce fuel slip. As the molar ratio of oxygen to methanol is increased, both reactant conversion and product yield increase in an almost linear fashion. At very higher molar ratios of oxygen to methanol, methanol can be converted efficiently to hydrogen, as the conversion accompanying with the reaction is nearly complete and the hydrogen yield is high. As the oxygen-methanol molar ratio is increased, the hydrogen productivity and output power of the reactor increase significantly in an almost linear fashion. The maximum hydrogen productivity and output power are obtained in the regime where the conversion is almost complete. To maximize the yield and productivity from the process, the molar ratio of oxygen to methanol must be controlled to match the stoichiometry of the reaction. The calculated output power of the reactor is of thousands of kilowatts or megawatts per cubic meter. However, there are practical limitations regarding the oxygen-methanol molar ratio. As the oxygen-methanol molar ratio is increased further, the temperature is raised to accelerate the reaction. Consequently, flames or explosion my occur, which will inevitably lead to very lower hydrogen productivity. The molar ratio of oxygen to methanol must be controlled precisely within certain needed limits to avoid the problems of combustion or explosion. The transition from combustion to explosion is caused by an acceleration of the reaction, induced either by a rise in temperature or by increasing lengths of the reaction chain. The first state is called thermal explosion, and the second state is called chain explosion. Thermal explosion theory is based on the idea that progressive heating raises the rate at which heat is released by the reaction until it exceeds the rate of heat loss from the area. At a given composition of the mixture and a given pressure, explosion will occur at a specific ignition temperature that can be determined from the calculations of heat loss and heat gain. It follows from the theory of branched-chain reactions that there is a limit to ignition, or to explosion, without a rise of temperature. In this case, what is called a chain explosion will occur when the probabilities of chain branching and of termination are equal.

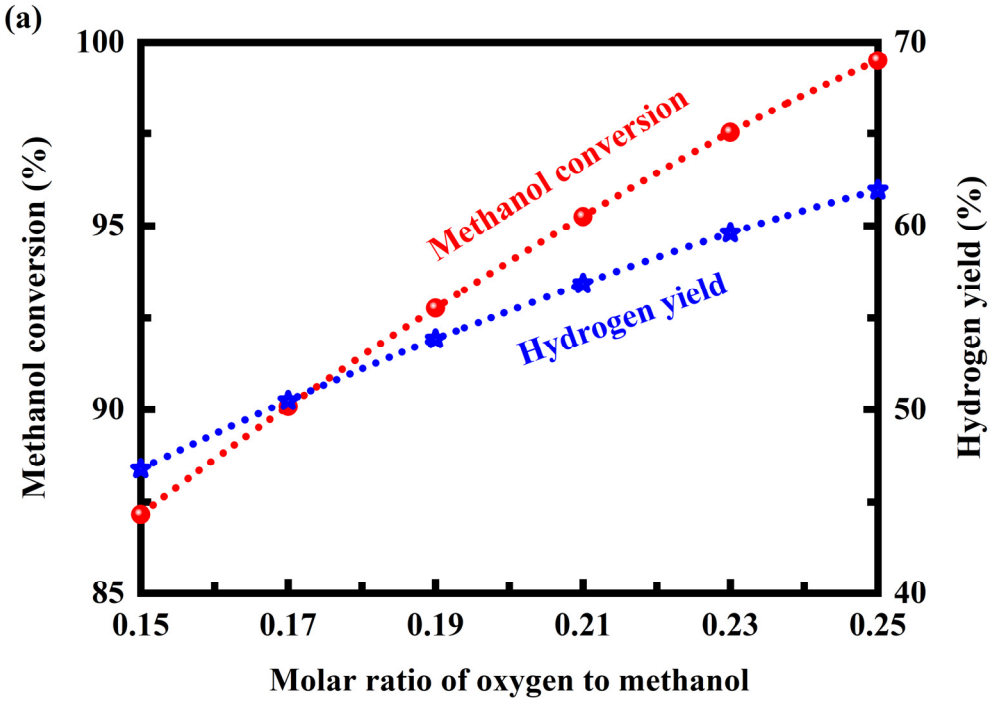

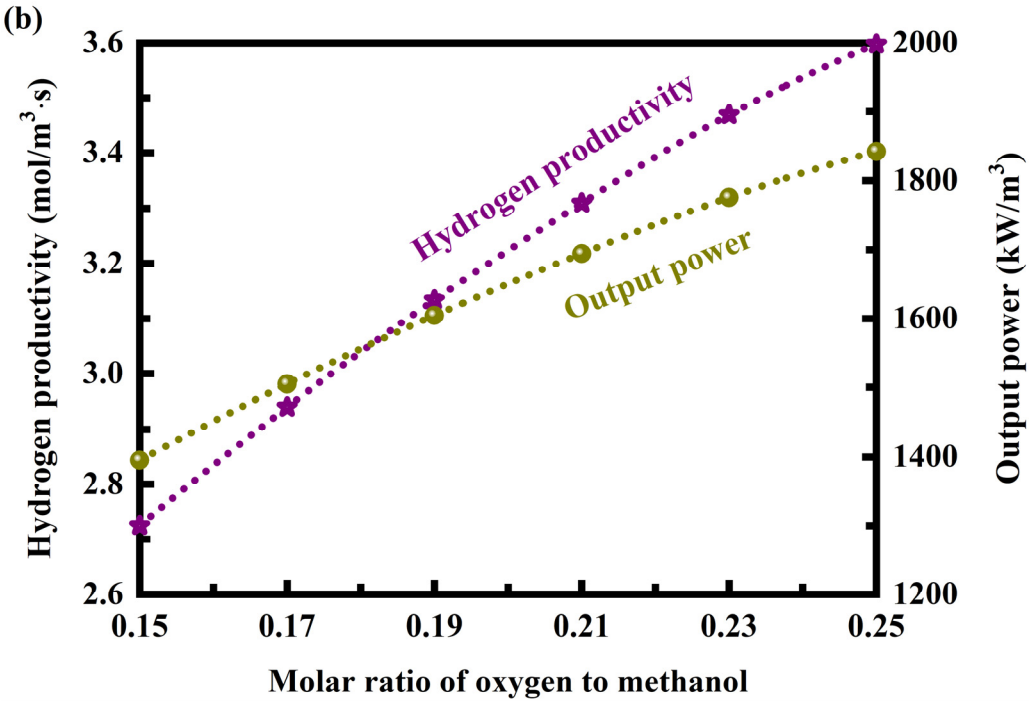

Figure 5. (a) Effects of the molar ratio of oxygen to methanol on the methanol conversion and hydrogen yield of the reactor. (b) Effects of the molar ratio of oxygen to methanol on the hydrogen productivity and output power of the reactor.

The two-dimensional contour maps of specific enthalpy, specific sensible enthalpy, and specific entropy in the reactor are illustrated in Figure 6 with the feed mixture at different molar ratios of oxygen to methanol. Enthalpy is the sum of the internal energy and the product of the pressure and volume of a thermodynamic system. Enthalpy is an energy-like property or state function. Its value is determined entirely by the temperature, pressure, and composition of the system. The specific enthalpy is entirely determined by the composition, pressure, and temperature of the reaction mixture. The specific sensible enthalpy refers to the energy absorbed by the reaction mixture to raise its temperature only. The specific entropy is determined completely by the current state of the reactor system. The specific enthalpy of the reaction mixture is substantially influenced by the oxygen-methanol molar ratio. In contrast, the feed composition has little effect on the specific sensible enthalpy and specific entropy of the reaction mixture. Consequently, the change in Gibbs free energy for the reaction is determined almost entirely by the change in specific enthalpy. The direction of the reaction is always toward a state of lower Gibbs free energy or specific enthalpy for the reactor system.

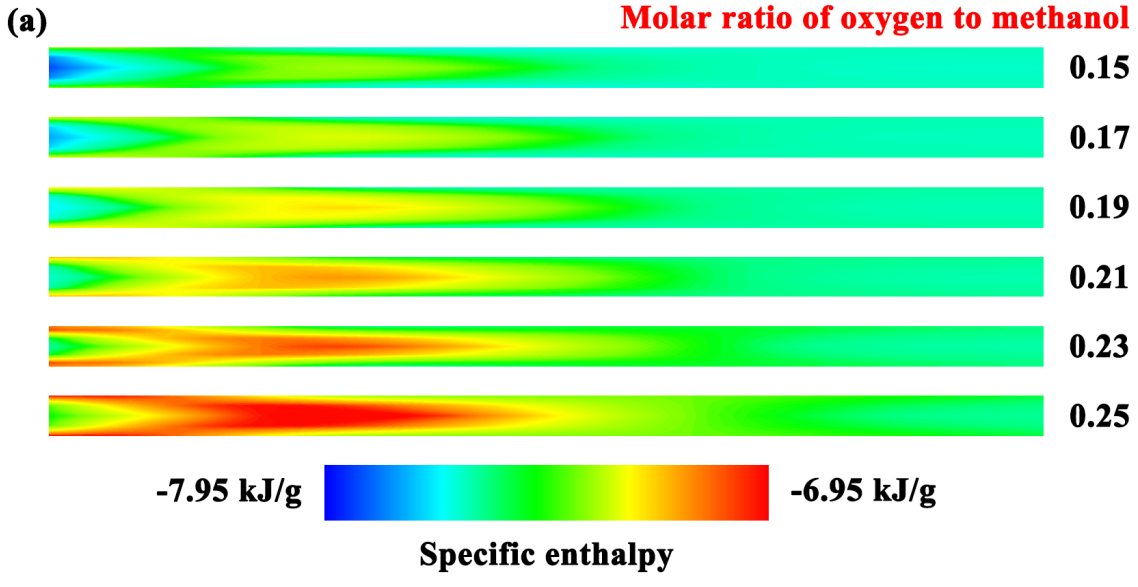

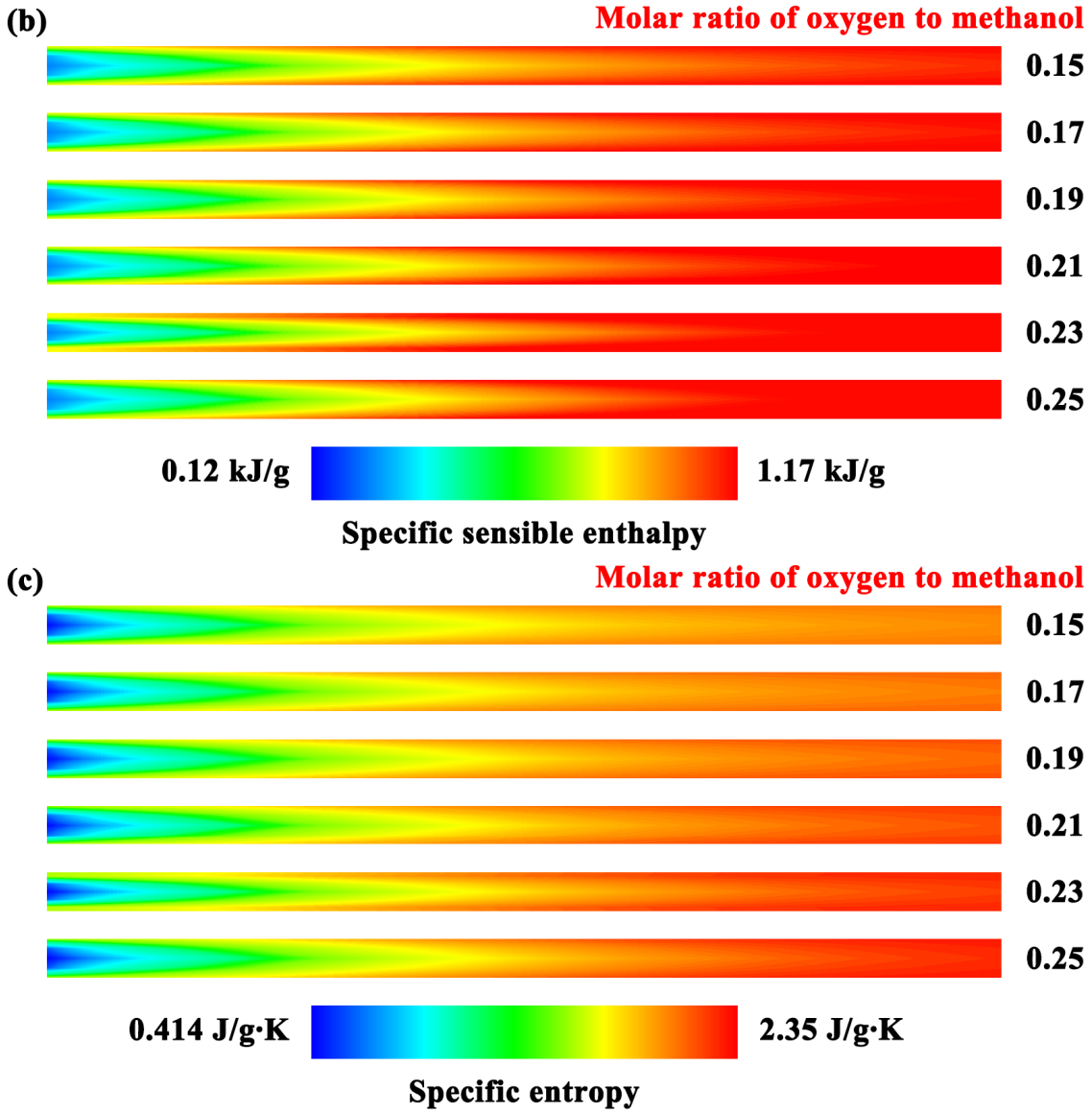

Figure 6. (a) Two-dimensional contour maps of specific enthalpy in the reactor with the feed mixture at different molar ratios of oxygen to methanol. (b) Two-dimensional contour maps of specific sensible enthalpy in the reactor with the feed mixture at different molar ratios of oxygen to methanol. (c) Two-dimensional contour maps of specific entropy in the reactor with the feed mixture at different molar ratios of oxygen to methanol.

The specific enthalpy and specific sensible enthalpy profiles along the channel centreline are presented in Figure 7 with the feed mixture at different molar ratios of oxygen to methanol. The enthalpy equals the sum of the internal energy and the product of the pressure and volume of the system. As with other energy functions, it is neither convenient nor necessary to determine absolute values of enthalpy. For each substance, the zero-enthalpy state can be some convenient reference state. The condition of minimum net specific enthalpy change for the reactor system is held at the highest molar ratio of oxygen to methanol. More specifically, the net specific enthalpy change is negative for the autothermal reforming reaction, if the feed mixture has an oxygen-methanol molar ratio of 0.25. In this case, the maximum conversion is attained and the autothermal reforming reaction is almost completed, as discussed above. In contrast, the net specific enthalpy change accompanying with the autothermal reforming reaction is positive or tends to zero, if the feed mixture has an oxygen-methanol molar ratio of no greater than 0.23. In these cases, methanol cannot be converted efficiently to hydrogen and therefore the hydrogen yield is relatively low. The condition of minimum net specific enthalpy change determines the maximum possible efficiency of the chemical process. The net specific

enthalpy change represents the fundamental limitation on how much heat can be extracted and converted for the autothermal reforming reaction.

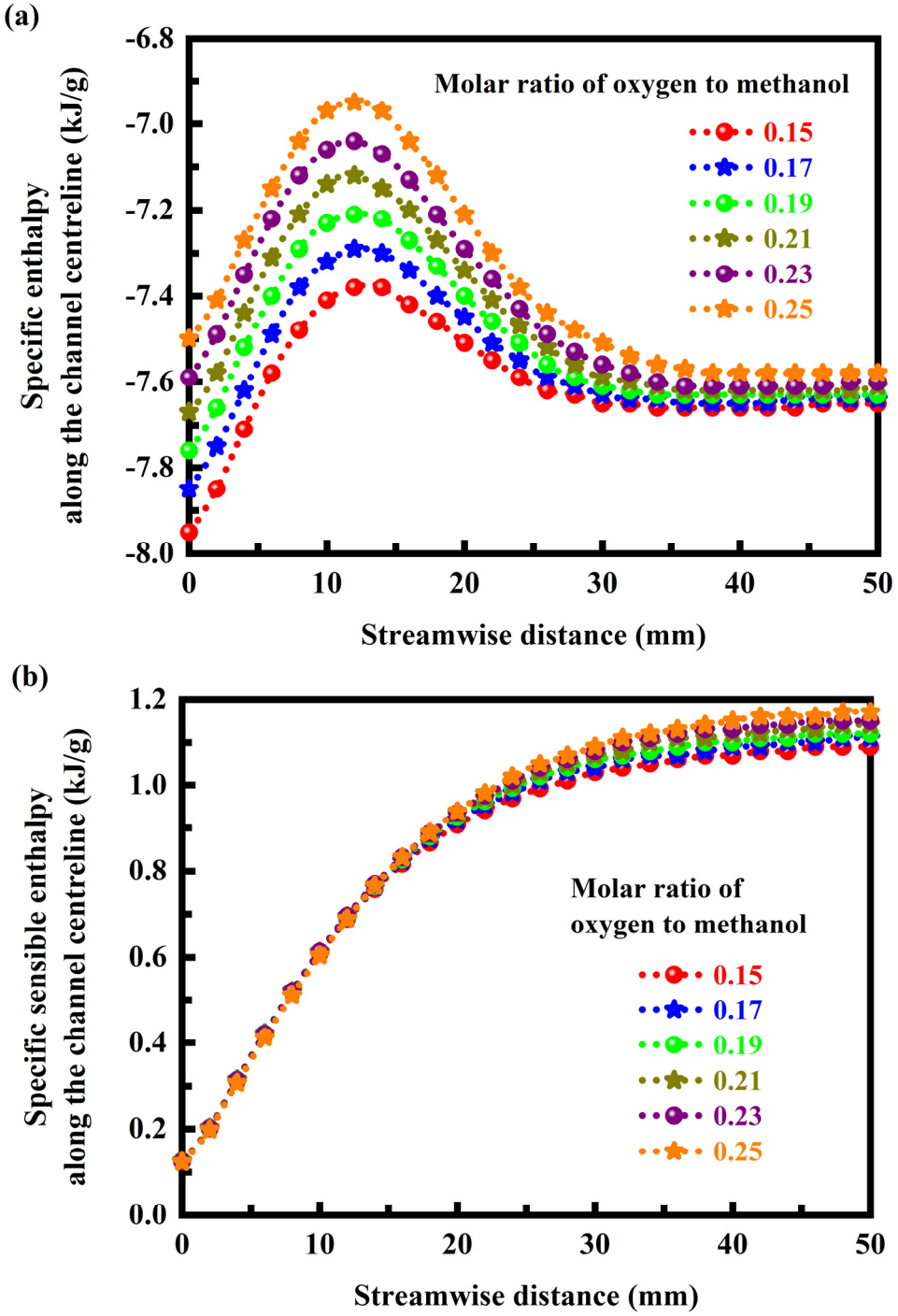

Figure 7. (a) Effect of the molar ratio of oxygen to methanol on the specific enthalpy along the channel centreline. (b) Effect of the molar ratio of oxygen to methanol on the specific sensible enthalpy along the channel centreline.

The behaviour of a complex thermodynamic system can be understood by applying the principles of states and properties to its component parts. The specific entropy profiles along the channel centreline of the autothermal reforming reactor are presented in Figure 8 with the feed mixture at different molar ratios of oxygen to methanol. For the autothermal reforming process, the feed composition has little effect on the specific entropy of the reaction mixture, especially near the entrance of the reactor. Additionally, the difference in the specific entropy of the reaction mixture between different molar ratios of oxygen to methanol is also small near the exit of the reactor. The concept of entropy provides deep insight into the direction of spontaneous change for the reaction phenomena. The

idea of entropy provides a mathematical way to encode the intuitive notion of which processes are impossible, even though they would not violate the fundamental law of conservation of energy. Entropy is an extensive property in that its magnitude depends on the amount of material in the system. The entropy of a closed system, or heat energy per unit temperature, increases over time toward some maximum value. Consequently, all closed systems tend toward an equilibrium state in which entropy is at a maximum and no energy is available to do useful work. The entropy of a perfect crystal of an element in its most stable form tends to zero as the temperature approaches absolute zero. This allows an absolute scale for entropy to be established that, from a statistical point of view, determines the degree of randomness or disorder in a system.

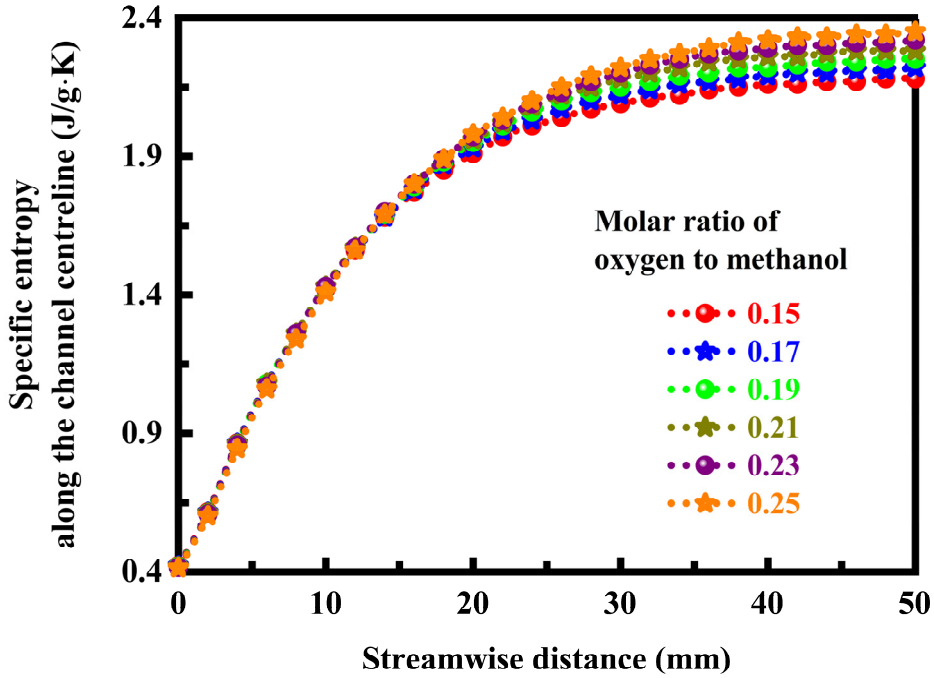

Figure 8. Effect of the molar ratio of oxygen to methanol on the specific entropy along the channel centreline of the autothermal reforming reactor.

4. Conclusions

Computational modelling for microchannel reactor design was conducted in the attempt to fully understand autothermal reforming phenomena in millisecond reactors. The effect of feed composition was investigated by means of various efficiency and performance criteria. Thermodynamic analysis was performed to describe the changes in the energy state of the reactor system.

The main conclusions are summarized as follows: Operation of the reactor is feasible at millisecond contact times. However, it is essential to balance the reactor efficiency and performance by optimising reaction conditions. The conversion to hydrogen is influenced greatly by the oxygen-methanol molar ratio. At the highest molar ratio of oxygen to methanol, the conversion is almost complete. However, equilibrium is not attained, as the methanol mole fraction is still slightly decreased near the exit of the reactor. To maximize the hydrogen yield and productivity from the chemical process, the oxygen-methanol molar ratio must be controlled to match the stoichiometry of the autothermal reforming reaction. However, it must be controlled precisely within certain needed limits to avoid the problems of combustion or explosion. Flames or explosion my occur, which will inevitably lead to very lower hydrogen productivity. The efficiency difference between feed compositions is determined by thermodynamic analysis. The calculated output power of the reactor is of the order of thousands of kilowatts per cubic meter.

References

[1] B.N. Iyke. Climate change, energy security risk, and clean energy investment. *Energy Economics*, Volume 129, 2024, Article Number: 107225.

[2] P.K. Narayan. Pricing behavior of clean energy stocks? Some trading implications. *Energy Economics*, Volume 134, 2024, Article Number: 107590.

[3] M.S. Dresselhaus and I.L. Thomas. Alternative energy technologies. *Nature*, Volume 414, Issue 6861, 2001, Pages 332-337.

[4] D. Larcher and J-M. Tarascon. Towards greener and more sustainable batteries for electrical energy storage. *Nature Chemistry*, Volume 7, Issue 1, 2015, Pages 19-29.

[5] N.Z. Muradov and T.N. Veziroğlu. From hydrocarbon to hydrogen-carbon to hydrogen economy. *International Journal of Hydrogen Energy*, Volume 30, Issue 3, 2005, Pages 225-237.

[6] N.Z. Muradov and T.N. Veziroğlu. "Green" path from fossil-based to hydrogen economy: An overview of carbon-neutral technologies. *International Journal of Hydrogen Energy*, Volume 33, Issue 23, 2008, Pages 6804-6839.

[7] S. Anwar, F. Khan, Y. Zhang, and A. Djire. Recent development in electrocatalysts for hydrogen production through water electrolysis. *International Journal of Hydrogen Energy*, Volume 46, Issue 63, 2021, Pages 32284-32317.

[8] S.S. Kumar and H. Lim. An overview of water electrolysis technologies for green hydrogen production. *Energy Reports*, Volume 8, 2022, Pages 13793-13813.

[9] D.R. Palo, R.A. Dagle, and J.D. Holladay. Methanol steam reforming for hydrogen production. *Chemical Reviews*, Volume 107, Issue 10, 2007, Pages 3992-4021.

[10] S.-S. Wang, X.-K. Gu, H.-Y. Su, and W.-X. Li. First-principles and microkinetic simulation studies of the structure sensitivity of Cu catalyst for methanol steam reforming. *The Journal of Physical Chemistry C*, Volume 122, Issue 20, 2018, Pages 10811-10819.

[11] B.C.H. Steele and A. Heinzel. Materials for fuel-cell technologies. *Nature*, Volume 414, Issue 6861, 2001, Pages 345-352.

[12] S. Chu and A. Majumdar. Opportunities and challenges for a sustainable energy future. *Nature*, Volume 488, Issue 7411, 2012, Pages 294-303.

[13] L.E. Bell. Cooling, heating, generating power, and recovering waste heat with thermoelectric systems. *Science*, Volume 321, Issue 5895, 2008, Pages 1457-1461.

[14] C. Wu. Analysis of waste-heat thermoelectric power generators. *Applied Thermal Engineering*, Volume 16, Issue 1, 1996, Pages 63-69.

[15] G.P. Sims. Hydroelectric energy. *Energy Policy*, Volume 19, Issue 8, 1991, Pages 776-786.

[16] A.U. Sarkar and S. Karagöz. Sustainable development of hydroelectric power. *Energy*, Volume 20, Issue 10, 1995, Pages 977-981.

[17] T. Jamal, G.M. Shafiullah, F. Dawood, A. Kaur, M.T. Arif, R. Pugazhendhi, R.M. Elavarasan, and S.F. Ahmed. Fuelling the future: An in-depth review of recent trends, challenges and opportunities of hydrogen fuel cell for a sustainable hydrogen economy. *Energy Reports*, Volume 10, 2023, Pages 2103-2127.

[18] K. Chaudhary, K. Bhardvaj, and A. Chaudhary. A qualitative assessment of hydrogen generation techniques for fuel cell applications. *Fuel*, Volume 358, Part A, 2024, Article Number: 130090.

[19] D.A. Cullen, K.C. Neyerlin, R.K. Ahluwalia, R. Mukundan, K.L. More, R.L. Borup, A.Z. Weber, D.J. Myers, and A. Kusoglu. New roads and challenges for fuel cells in heavy-duty transportation. *Nature Energy*, Volume 6, Issue 5, 2021, Pages 462-474.

[20] K. Jiao, J. Xuan, Q. Du, Z. Bao, B. Xie, B. Wang, Y. Zhao, L. Fan, H. Wang, Z. Hou, S. Huo, N.P. Brandon, Y. Yin, and M.D. Guiver. Designing the next generation of proton-exchange membrane

fuel cells. *Nature*, Volume 595, Issue 7867, 2021, Pages 361-369.
[21] Z. Xin, Z. Yanyi, and W. Xiaobing. Research on testing and evaluation technology of proton exchange membrane for fuel cell. *Energy Reports*, Volume 10, 2023, Pages 1943-1950.
[22] J. Shin, M. Son, S.-I. Kim, S.A. Song, and D.H. Lee. Design of multi-layered gradient catalysts for efficient proton exchange membrane fuel cells. *Journal of Power Sources*, Volume 582, 2023, Article Number: 233546.
[23] P. Halder, M. Babaie, F. Salek, N. Haque, R. Savage, S. Stevanovic, T.A. Bodisco, and A. Zare. Advancements in hydrogen production, storage, distribution and refuelling for a sustainable transport sector: Hydrogen fuel cell vehicles. *International Journal of Hydrogen Energy*, Volume 52, Part D, 2024, Pages 973-1004.
[24] S. Bhogilla, A. Pandoh, and U.R. Singh. Cogeneration system combining reversible PEM fuel cell, and metal hydride hydrogen storage enabling renewable energy storage: Thermodynamic performance assessment. *International Journal of Hydrogen Energy*, Volume 52, Part D, 2024, Pages 1147-1155.
[25] L. Alejo, R. Lago, M.A. Peña, and J.L.G. Fierro. Partial oxidation of methanol to produce hydrogen over Cu-Zn-based catalysts. *Applied Catalysis A: General*, Volume 162, Issues 1-2, 1997, Pages 281-297.
[26] R. Ubago-Pérez, F. Carrasco-Marín, and C. Moreno-Castilla. Methanol partial oxidation on carbon-supported Pt and Pd catalysts. *Catalysis Today*, Volume 123, Issues 1-4, 2007, Pages 158-163.
[27] P.J. Dauenhauer, J.R. Salge, and L.D. Schmidt. Renewable hydrogen by autothermal steam reforming of volatile carbohydrates. *Journal of Catalysis*, Volume 244, Issue 2, 2006, Pages 238-247.
[28] T. Hos, G. Sror, and M. Herskowitz. Autothermal reforming of methanol for on-board hydrogen production in marine vehicles. *International Journal of Hydrogen Energy*, Volume 49, Part A, 2024, Pages 1121-1132.
[29] D.W. Agar. Multifunctional reactors: Old preconceptions and new dimensions. *Chemical Engineering Science*, Volume 54, Issue 10, 1999, Pages 1299-1305.
[30] R. Krishna and S.T. Sie. Strategies for multiphase reactor selection. *Chemical Engineering Science*, Volume 49, Issue 24, Part A, 1994, Pages 4029-4065.
[31] J.D. Holladay, Y. Wang, and E. Jones. Review of developments in portable hydrogen production using microreactor technology. *Chemical Reviews*, Volume 104, Issue 10, 2004, Pages 4767-4790.
[32] D. Yadav, X. Lu, C.B. Vishwakarma, and D. Jing. Advancements in microreactor technology for hydrogen production via steam reforming: A comprehensive review of experimental studies. *Journal of Power Sources*, Volume 585, 2023, Article Number: 233621.
[33] F. Nalchifard and A. Sari. Thermal coupling of methanol steam reforming and hydrogen combustion to produce fuel cell hydrogen: A comparative theoretical study between membrane and hydrogen-recycled shell-and-tube reactors. *Fuel*, Volume 357, Part B, 2024, Article Number: 129826.
[34] X. Mao, W.Z. Li, Y. Yuan, and L.W. Yang. Numerical analysis of methanol steam reforming reactor heated by catalytic combustion for hydrogen production. *International Journal of Hydrogen Energy*, Volume 47, Issue 32, 2022, Pages 14469-14482.
[35] T. Zheng, W. Zhou, X. Li, H. You, Y. Yang, W. Yu, C. Zhang, X. Chu, K.S. Hui, and W. Ding. Structural design of self-thermal methanol steam reforming microreactor with porous combustion reaction support for hydrogen production. *International Journal of Hydrogen Energy*, Volume 45, Issue 43, 2020, Pages 22437-22447.
[36] M. Mundhwa and C.P. Thurgood. Numerical study of methane steam reforming and methane

combustion over the segmented and continuously coated layers of catalysts in a plate reactor. *Fuel Processing Technology*, Volume 158, 2017, Pages 57-72.

[37] R.C. Ramaswamy, P.A. Ramachandran, and M.P. Duduković. Recuperative coupling of exothermic and endothermic reactions. *Chemical Engineering Science*, Volume 61, Issue 2, 2006, Pages 459-472.

[38] R.C. Ramaswamy, P.A. Ramachandran, and M.P. Duduković. Coupling exothermic and endothermic reactions in adiabatic reactors. *Chemical Engineering Science*, Volume 63, Issue 6, 2008, Pages 1654-1667.

[39] P. Vadasz. On the paradox of heat conduction in porous media subject to lack of local thermal equilibrium. *International Journal of Heat and Mass Transfer*, Volume 50, Issues 21-22, 2007, Pages 4131-4140.

[40] A. Gandomkar and K.E. Gray. Local thermal non-equilibrium in porous media with heat conduction. *International Journal of Heat and Mass Transfer*, Volume 124, 2018, Pages 1212-1216.

[41] K. Boomsma and D. Poulikakos. On the effective thermal conductivity of a three-dimensionally structured fluid-saturated metal foam. *International Journal of Heat and Mass Transfer*, Volume 44, Issue 4, 2001, Pages 827-836.

[42] A. Nakayama. Effective thermal conductivity of porous media. *Advances in Heat Transfer*, Volume 56, 2023, Pages 51-111.

[43] E. Santacesaria and S. Carrá. Kinetics of catalytic steam reforming of methanol in a CSTR reactor. *Applied Catalysis*, Volume 5, Issue 3, 1983, Pages 345-358.

[44] J.C. Amphlett, R.F. Mann, and B.A. Peppley. The steam reforming of methanol: mechanism and kinetics compared to the methanol synthesis process. *Studies in Surface Science and Catalysis*, Volume 81, 1994, Pages 409-411.

[45] J.T. Richardson. A gas fired heat-pipe reformer for small-scale hydrogen production. *Studies in Surface Science and Catalysis*, Volume 107, 1997, Pages 567-571.

[46] J. Sogge and T. Strom. Membrane reactors-a new technology for production of synthesis gas by steam reforming. *Studies in Surface Science and Catalysis*, Volume 107, 1997, Pages 561-566.